BIOLOGY OF REPRODUCTION **59,** 1240–1250 (1998)

Characterization of a Major Permeability Barrier in the Zebrafish Embryo[1]

Mary Hagedorn,[2,3] F.W. Kleinhans,[4] Dmitri Artemov,[5] and Ulrich Pilatus[5]

Reproductive Physiology Program,[3] National Zoological Park, Smithsonian Institution, Washington, District of Columbia 20008
Physics Department,[4] IUPUI, Indianapolis, Indiana 46202
Radiology Department,[5] Johns Hopkins School of Medicine, Baltimore, Maryland 21205

ABSTRACT

Fish embryos represent a class of multicompartmental biological systems that have not been successfully cryopreserved, primarily because of the lack of understanding of how water and cryoprotectants permeate the compartments. We are using the zebrafish embryo as a model to understand these kinetics. Zebrafish embryos have two major compartments, the blastoderm and the yolk, which is surrounded by the multinucleated yolk syncytial layer (YSL). We determined the water and cryoprotectant permeability in these compartments using two methods. First, we measured shrink/swell dynamics in optical volumetric experiments. Zebrafish embryos shrank over time and did not re-expand while immersed in dimethyl sulfoxide (DMSO) or propylene glycol. Second, we measured DMSO uptake with diffusion-weighted nuclear magnetic resonance spectroscopy. DMSO uptake was rapid during the first few minutes, then gradual thereafter. We used one- and two-compartment models to analyze the data and to determine the permeability parameters. We found that the two-compartment model provided a better fit to the data. On the basis of this model and in the presence of DMSO, the yolk and blastoderm had very similar water permeabilities (i.e., 0.01 and 0.005 $\mu m \times min^{-1}atm^{-1}$, respectively), but they had different DMSO permeabilities separated by three orders of magnitude (i.e., $\leq 5 \times 10^{-6}$ and 1.5×10^{-3} cm/min, respectively). The low solute permeability of the yolk predicted that the yolk/YSL compartment should be more susceptible to cryodamage. To test this, the yolk, blastoderm, and YSL were examined at the ultrastructural level after vitrification. Only the YSL incurred significant damage after freezing and thawing ($p \leq 0.05$).

INTRODUCTION

Yolk-laden embryos of fish, reptiles, birds, and amphibians represent a class of multicompartmental biological systems that have not been successfully cryopreserved. Over the past 50 years, the fish embryo has presented a challenge to cryobiologists because of its interesting and complex physiology. Successful cryopreservation of fish embryos must address several important issues, including 1) the intrinsic biophysical properties of the cells (e.g., membrane permeabilities and osmotic tolerance limits) and 2) determination of the procedural cryopreservation steps, based on the cell's biophysical properties, necessary to minimize cryodamage and maximize survival [1]. In this paper, we examine the kinetics of cryoprotectant permeability of the yolk and blastoderm compartments, and the effects of cryodamage on the fish embryo.

We are using the zebrafish embryo as a model to understand the cryobiological properties of a multicompartmental system. The zebrafish model is becoming one of the most important vertebrate models for the study of development and genetics. Transgenic and mutagenic studies of zebrafish are expected to play an important role in human health and disease. The human genome is being mapped, but the functionality of many of the genes is not known. On the other hand, the function of many of the genes in the zebrafish genome is known because of the mutational screens going on in a number of labs throughout the world. When the zebrafish genome is fully mapped (hopefully within the next few years), it will have great value, because the organization of the fish and human genomes has been relatively conserved throughout evolution [2]. Therefore, cryopreservation of this embryo would be a great service to the field. The zebrafish embryo is composed of two cellular compartments: a large yolk and the developing blastoderm (Fig. 1). The major component of the yolk is vitellogenin, a large phospholipid (approximately 400 kDa; [3]), stored in membrane-bound vesicles within the yolk. The major developmental stages important for this work are 100% epiboly to the 3-somite stage. We did not consider earlier developmental stages, because they are sensitive to chilling [4, 5] and are mechanically fragile, thus making them less attractive for cryopreservation. At the onset of development, the blastoderm divides and forms a cap of cells on the large yolk. At the 128-cell stage, epiboly begins as the blastoderm envelopes the yolk and ceases once the yolk is completely surrounded by blastoderm at 100% epiboly [6]. Underlying the blastoderm and covering the yolk is the yolk syncytial layer (YSL). This is a multinucleated layer (approximately 10 μm thick) of nonyolky cytoplasm that begins to develop at approximately the 1000-cell stage in the zebrafish embryo [7]. As the YSL develops, it replaces the thin (approximately 2 μm thick), nonnucleated yolk cytoplasmic layer [8]. The YSL begins to envelop the yolk ahead of the blastoderm, and it surrounds the embryo by approximately 50–75% epiboly [9]. The segmentation period follows. The stages within this period are identified by the number of muscle somites visible in the tail region from the 1- to the 26-somite stage.

The efficacy of cryoprotectant permeation is crucial to formulating successful cryopreservation procedures. Each compartment may have different permeability to water and cryoprotectants. To prevent cryodamage, the compartment with the lowest permeability to water and cryoprotectant must be considered when formulating cryopreservation procedures. Much of the work to date on cryoprotectant permeability of the teleost embryo has not addressed the embryo's multicompartmental nature. Harvey et al. [10] examined the permeability of zebrafish embryos at 50% epib-

Accepted July 8, 1998.
Received May 14, 1998.
[1]Supported by grants from the National Institutes of Health (R29 RR08769) (M.H.), and Maryland Sea Grant College (M.H.), and from IUPUI for a Sabbatical Year Award (F.W.K.), and the Smithsonian Institution for a Smithsonian Short-Term Visitor Award (F.W.K.).
[2]Correspondence: M. Hagedorn, National Zoological Park, Smithsonian Institution, 3001 Conn. Ave., NW, Washington, DC 20008. FAX: 202 673 4733; e-mail: mhagedorn@nzp.si.edu

Downloaded from https://academic.oup.com/biolreprod/article/59/5/1240/2741051 by guest on 16 August 2022

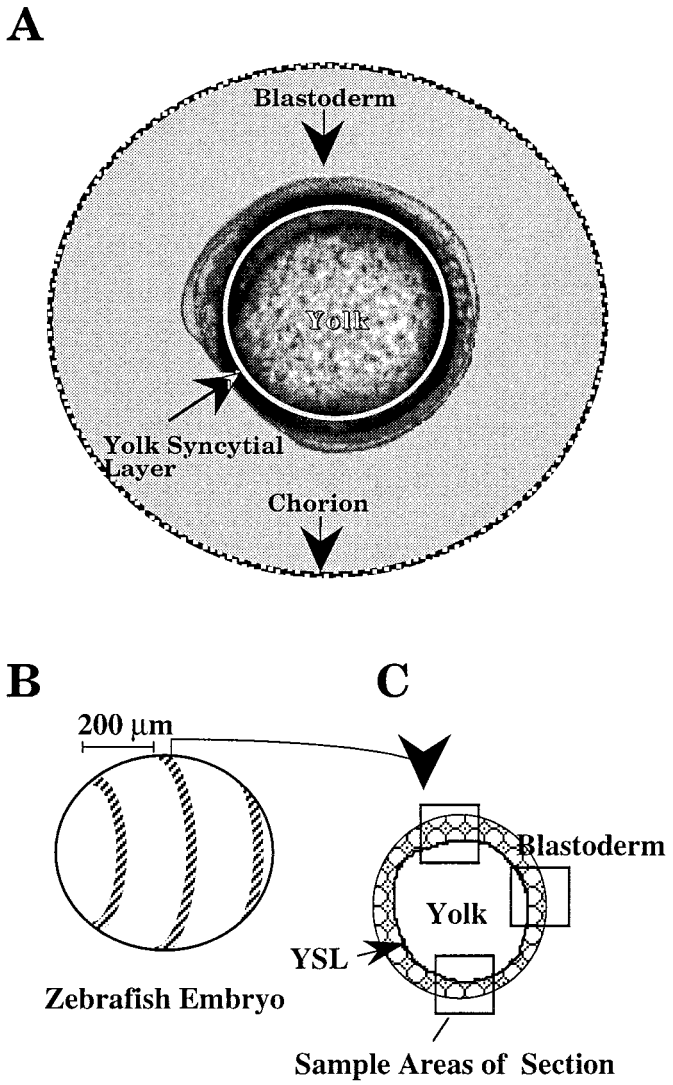

FIG. 1. **A**) Image of a zebrafish embryo identifying the major compartments (i.e., yolk and blastoderm). Although the YSL normally would not be visible, its position is indicated on the embryo for clarity. The position of the chorion is indicated even though this layer was removed in all of our preparations. **B** and **C**) Method of sampling the zebrafish embryo for ultrastructural analysis. **B**) Locations from which thin sections were sampled from the whole embryo. **C**) Location on the thin section where areas of the blastoderm, YSL, and yolk were examined for ultrastructural integrity.

oly to isotope-labeled glycerol and dimethyl sulfoxide (DMSO). He found that DMSO permeated into dechorionated embryos and that both solutes permeated into intact embryos. Unfortunately, the amount and location (i.e., yolk versus blastoderm) of these permeating cryoprotectants were unclear. Subsequently, Harvey [11] reported that glycerol protected only the blastoderm, and neither cryoprotectant effectively preserved the entire embryo at −196°C. Recently, Suzuki et al. ([12]; for carp, medaka, and rainbow trout) and Lubzens et al. ([13]; for carp) reported an uptake of DMSO solution into the perivitelline space and some tissues, but the permeation level was insufficient for cryopreservation. Using optical measurements, Zhang and Rawson [14, 15] described cryoprotectant permeation into intact and dechorionated zebrafish embryos. Of the variety of cryoprotectants that they tried, only methanol showed clear evidence of permeation into the embryos.

We have examined the multicompartmental zebrafish embryo using a variety of techniques that can reveal the permeability response of the individual compartments [16, 17]. These experiments identified the YSL as a barrier to the movement of cryoprotectants into the yolk. Specifically, little or no DMSO or propylene glycol (PG) entered the yolk, but methanol did. Unfortunately, methanol may not be a suitable cryoprotectant for vitrification (a method needed because of the embryo's chill sensitivity), whereas DMSO and PG may. Our previous studies [16] identified the existence and location of the permeability barrier to DMSO and PG, whereas the present study quantified the water and solute permeability parameters for the yolk and blastoderm. We used two methods to estimate the permeability parameters. First we measured cryoprotectant-induced volumetric changes by light microscopic analysis and then cryoprotectant uptake with diffusion-weighted ^{1}H nuclear magnetic resonance (NMR) spectroscopy. Nonlocalized NMR spectroscopy was selected for this study instead of single-embryo NMR microscopy, as used previously [16], because a larger sample size could be used. This increased the signal-to-noise; therefore, smaller amounts of cryoprotectants could be detected within the embryos.

When a single cell is exposed to a hyperosmotic solute solution (e.g., 2 M DMSO or 2 M PG), water initially leaves the cell and solute enters the cell in response to the osmotic and solute gradients. Eventually, as the intracellular solute concentration rises, water re-enters the cell, producing the typical shrink-swell volume curves seen in many optical experiments. The rate at which the cell volume changes in response to the water and solute flux reflects the permeability of the cell membrane to water and solute. These parameters are characterized by the hydraulic or water permeability (L_p) and solute permeability (P_s), respectively. In order to determine permeability parameters for the multicompartmental zebrafish embryo from the NMR and optical data, it is necessary to have a model of the embryo. Initially we considered a one-compartment model and then generalized to a more complex two-compartment model. For modeling purposes, we did not distinguish the YSL from the yolk and consider it part of the yolk compartment.

As stated earlier, all attempts to cryopreserve fish embryos have produced lethal damage. This analysis of the permeability parameters of the zebrafish embryo predicted that a major site of the lethal cryodamage would occur within the yolk compartment. Presumably, without sufficient cryoprotectant entering the yolk, damaging ice-crystals form. To test this hypothesis, we vitrified zebrafish embryos and examined the cellular ultrastructure of the cryodamage in the blastoderm and the yolk compartments.

MATERIALS AND METHODS

Maintenance of Animals

Animals were maintained according to the maintenance and culturing procedures described by Westerfield [6]. Briefly, 12–16 fish were kept in 5-L aquaria (temp = 28.5°C; pH = 7.0) illuminated according to a 12L:12D cycle, and fed dried copepods and krill (Argent Laboratories, Redmond, WA). Animals spawned in response to photoperiod, producing 50–60 embryos per female. Embryos were collected, dechorionated by enzymatic digestion, and maintained in embryo medium (a modified Hepes buffer at 0.040 Osm) as described in Westerfield [6]. All solutions were made up in this embryo medium. Because the devel-

Downloaded from https://academic.oup.com/biolreprod/article/59/5/1240/2741051 by guest on 16 August 2022

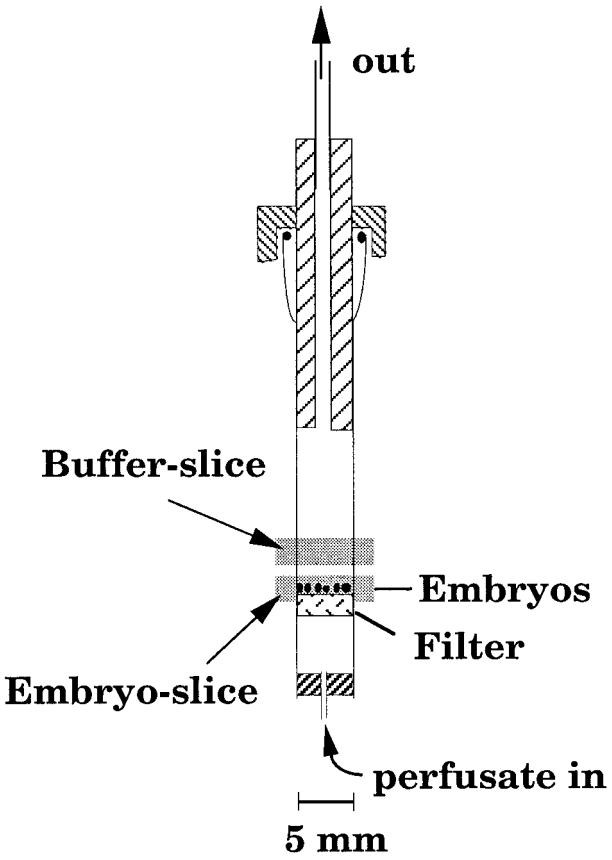

FIG. 2. NMR perfusion sample chamber. Diagram of the experimental perfusion set-up and location of the NMR slices selected for the experiment.

opmental temperature was 28.5°C, all developmental stages described here are similar to those in Westerfield [6].

Throughout the study, only embryos at 100% epiboly to the 3-somite stage were used. At this time, there was no epidermis covering the embryo that might act as a diffusion barrier by hindering permeability to water and cryoprotectants. Moreover, embryos still were relatively round, maintained a reproducible orientation when moved from solution to solution, and were nonmotile, simplifying the optical volumetric measurements.

Volumetric Measurements: Light Microscopy

After immersion in a hypertonic solute (2 M DMSO or PG in embryo medium), changes in embryo size were measured using computer-assisted light microscopy. Embryos were examined under a Zeiss compound microscope fitted with a CCD camera (WV-BL200; Panasonic, Secaucus, NJ) at room temperature (approximately 22°C). Images were digitized with a video frame-grabber card (LG3; Scion Corp., Frederick, MD) and stored for later morphometric analysis. Digitized images (×100) were displayed on a high-resolution video monitor and analyzed using a computer-aided morphometry package (Image 1.45; NIH, Bethesda, MD). The outline of each embryo was determined by the computer, and linear, planar, and volumetric parameters of each embryo were calculated. The major and minor axes were used to determine the volume of embryos at all stages using a prolate spheroid formula ($V = 4/3\pi\ ab^2$), where a and b were the major and minor semi-axes, respectively. The data were modeled as described below.

Solute Uptake: NMR Spectroscopy

NMR data were acquired on an Omega 400 NMR (General Electric, Fremont, CA) spectrometer (equipped with GE Accustar actively shielded gradients up to 130 G/cm in three directions) using a specially designed probe for perfusion experiments with 5-mm NMR tubes. Embryos (each sample consisted of 20 embryos at 100% epiboly) rested as a monolayer on a porous filter (Fritware; Bel-Art Products, Pequannock, NJ, polyethylene sheets, 70-micron pore size, 3.2 mm thickness) placed in a bottom-cut 5-mm NMR tube (Fig. 2). Embryo medium was pumped through the NMR tube, perfusing the embryos from below at 0.3 ml/min with a peristaltic pump (Masterflex; Cole-Palmer, Vernon Hills, IL) for 20 min and was then changed to 2.0 M DMSO for 60 min. To follow any rapid changes in the embryos, localized spectra (two scans/spectrum, 1 sec repetition time) were acquired every 44 sec at two different cross-sectional locations in the NMR tube, one slice containing the embryos and the other in the solution just above the embryos (Fig. 2). ^{1}H-NMR spectra were obtained with stimulated echo pulse sequences using high and low diffusion-weighting with the spatial localization in the z direction (i.e., parallel to the NMR tube) obtained by slice selective radio frequency pulses following the methods of Frahm et al. [18].

NMR spectra of the slice containing the embryos were obtained with high diffusion-weighting, which was sufficient to suppress all extracellular water and DMSO, allowing only intracellular water and DMSO to be detected [16]. Low diffusion-weighted spectra were obtained in the upper buffer slice to show the time course of the appearance of DMSO in the buffer. The rate at which DMSO signal appeared in the buffer slice placed a lower limit on the measurable embryo response time. Changes in intracellular DMSO were obtained from the high diffusion-weighted spectra from the lower slice (embryo slice) and were quantified by measuring the change in area under the spectral peaks of the DMSO. Since the intensity of diffusion-weighted signals depends on many factors, such as relaxation processes that may interfere with quantification of intracellular DMSO, we were not able to measure the absolute intracellular quantity of DMSO. However, the signal intensity (area under the signal) is proportional to the quantity of intracellular DMSO. These intensities were arbitrarily normalized, and then three separate NMR runs were averaged to yield the data presented here. In all experiments, the embryos were counted before introduction and after removal from the magnet to insure that changes observed were due to physiological changes and not due to the embryo number diminishing during the experiment. Initially, NMR experiments were performed using PG. Unfortunately, a signal of an endogenous (unidentified) compound within the embryos appeared at approximately the same position as PG. This caused large errors in quantifying intracellular PG, especially when low concentrations had to be determined, so the PG NMR experiments were terminated. The DMSO data were modeled as described below.

Permeability Parameters

The objective of the modeling was to determine the permeability parameters of the zebrafish embryo from the optical and NMR data. In the optical experiments, we measured the changing embryo volume (V_c), which depends on the flux of water and solute into or out of the embryo. In

Downloaded from https://academic.oup.com/biolreprod/article/59/5/1240/2741051 by guest on 16 August 2022

the NMR experiments, we measured the (relative) quantity of solute taken up by the embryo as the number of moles of solute (N_s) in the embryo over time. The flux of water into a cell is determined by its water permeability or hydraulic conductivity (L_p). Experimentally, it is often found that L_p depends on whether the osmotic driving gradient is produced by a permeating (e.g., DMSO) or nonpermeating (e.g., NaCl) solute. To distinguish between these two cases, we referred to the water permeability in the presence of a permeating solute as L_p^s. The flux of solute into the cell is determined by the solute permeability (P_s). The task was to relate the permeability parameters L_p^s and P_s to V_c and N_s.

The embryo volume (V_c) is the sum of the water (V_w), solute (V_s), and solids (V_{solids}) volumes:

$$V_c = V_w + V_s + V_{solids} = V_w + M_s^i V_w \bar{V}_s + v_b V_{co}, \quad (1)$$

where v_b is the fractional volume of the osmotically inactive cell contents, $\bar{V}_s$ is the solute partial molar volume, and V_{co} is the isotonic volume of the cell. Thus the problem was reduced to one of finding the water volume (V_w) and the solute content (N_s) of the embryo. These two quantities were given by a pair of coupled, differential equations that must be numerically integrated along with subsidiary defining equations. These equations are outlined below.

The water flux into a cell is given by:

$$dV_w/dt = L_p^s ART(M^i - M^e), \quad (2)$$

where A is the cell surface area, R and T the gas constant and absolute temperature, respectively, and M^i and M^e are the intracellular and extracellular medium osmolality. The solute flux is given by:

$$dN_s/dt = P_s A(M_s^e - M_s^i), \quad (3)$$

where N_s is the number of osmoles of solute in the cell, and M_s^e and M_s^i are the extracellular and intracellular solute osmolalities, respectively. Sometimes it is more convenient to express the solute flux in terms of the intracellular solute osmolality ($M_s^i = N_s/V_w$). Substituting $V_w M_s^i$ for N_s in equation 3 and utilizing equation 2 yielded:

$$dM_s^i/dt = P_s(A/V_w)(M_s^e - M_s^i) + L_p^s(A/V_w)M_s^i RT(M^e - M^i). \quad (4)$$

The external medium osmolality (M^e) was set by the experimental conditions:

$$M^e = M_n^e + M_s^e, \quad (5)$$

where M_n^e is the external nonpermeating solute concentration and M_s^e is the external permeating solute concentration (DMSO or PG). The intracellular osmolality M^i was computed assuming a linear Boyle van't Hoff cell response:

$$M^i = M_{no}^i(V_{wo}/V_w) + M_s^i, \quad (6)$$

where the subscripts n, o, and w refer to nonpermeating solute, initial (t = 0) conditions, and water, respectively.

The cell volume (V_c) and intracellular solute (N_s) were modeled by simultaneously integrating equations 2 and 3 or equations 2 and 4. In the NMR experiments, only the relative solute concentration (N_{rel}) was measured; thus in equation 3, a scaling factor (S_f) must be introduced so that $N_s = S_f \times N_{rel}$. Integration was done using the Stiff Episode integrator in the program Scientist (MicroMath, Salt Lake City, UT). The permeability parameters, L_p^s and P_s (and S_f in the NMR experiment) were obtained by iteratively varying them until a good fit was obtained between the model calculations and the experimental observables, specifically V_c, N_{rel}, or V_c and N_{rel}. Least-squares fitting was performed using the Powell variant of the Levenberg-Marquardt method as implemented in the program Scientist. In some cases, a wide range of P_s values gave a satisfactory fit to the experimental data. In these cases, P_s was manually varied to find the acceptable range of values as judged by visual evaluation of the fits. A number of fixed parameters appear

TABLE 1. Parameters used for the one- and two-compartment model analyses of the NMR solute uptake and optical volume measurements; embryos were at approximately 100% epiboly for these experiments.

Parameter	Value	Comments
General parameters		
M_{no}^i	0.300 Osm	Assumed cytoplasmic and yolk osmolality.[a]
M_n^e	0.040 Osm	Osmolality of external, nonpermeating embryo medium.
M_s^e	2.39 Osm	Osmolality of external 2 M DMSO or 2 M PG.
$\bar{V}_s$ (DMSO)	0.069 l/mol	Partial molar volume of DMSO.
$\bar{V}_s$ (PG)	0.070 l/mol	Partial molar volume of PG.
T	294–296 K	Temperature of NMR and optical experiments.
One compartment model parameters		
V_o	0.2 mm^3	Volume of "standard" embryo.
A	1.65 mm^2	Area of "standard" embryo, assumed to be spherical.
v_b	0.36	Osmotically inactive fraction of embryo.[b]
L_p^s	variable	Hydraulic conductivity in presence of solute.
P_s	variable	Solute permeability.
Two compartment parameters		
V_o	0.2 mm^3	Volume of "standard" embryo.
f_y	0.77	Fraction of embryo volume that is yolk.[c]
f_b	0.23	Fraction of embryo volume that is blastoderm.[c]
A_y	1.39 mm^2	Assumed surface area of yolk compartment.[d]
A_b	1.65 mm^2	Surface area of blastoderm compartment.[d]
v_{by}	0.41	Osmotically inactive fraction of yolk.[e]
v_{bb}	0.20	Osmotically inactive fraction of blastoderm.[e]
L_{py}^s	variable	Hydraulic conductivity of yolk compartment in presence of solute.
L_{pb}^s	variable	Hydraulic conductivity of blastoderm compartment in presence of solute.
P_{sy}	variable	Solute permeability of yolk compartment.
P_{sb}	variable	Solute permeability of blastoderm compartment.

[a] The internal osmolality of the zebrafish is unknown. The embryos are held in embryo medium at 0.040 Osm. However, a number of arguments point to an internal embryo osmolality closer to 0.300 Osm. It is not understood how zebrafish embryos can regulate their internal osmotic environment while living in such a hypo-osmotic environment. Vapor pressure osmometer measurements suggest an osmolality of approximately 0.240 Osm (Hagedorn, unpublished data). We choose 0.300 Osm for these models to match the osmolality of a typical vertebrate cell.

[b] This is determined by adding together the components of the two-compartment model ($v_b = f_y \times v_{by} + f_b \times v_{bb}$).

[c] These fractional compartmental volumes are taken from measurements of the yolk and blastoderm as a function of developmental stage [5].

[d] At 100% epiboly, the embryo has an approximately spherical yolk compartment surrounded by a thin layer of blastoderm cells. The area of the blastoderm compartment is taken to be just the outer surface area of the embryo, assuming a spherical volume. The yolk compartment is a sphere of somewhat smaller size (containing 77% of the volume), with a surface area of 1.39 mm^2.

[e] Hagedorn et al. [17], see text.

Downloaded from https://academic.oup.com/biolreprod/article/59/5/1240/2741051 by guest on 16 August 2022

in the fitting equations, and their values are listed in Table 1. Some justifications for the fixed parameter values appear in the next section.

Typical initial volumes of 100% epiboly embryos (or slightly larger) in the optical experiments were observed to scatter approximately at 0.20 mm^3. Therefore, all initial volumes were normalized to this value. Further, all data for a given experimental series were averaged before fitting to reduce noise and reduce the computational burden. In the NMR experiments, the data were first (arbitrarily) normalized, then averaged.

Modeling the Zebrafish Embryo

Two different structural models were used in fitting the data. The simpler was a one-compartment model assuming a spherical embryo of initial volume 0.20 mm^3 with a fixed area of 1.65 mm^2 and an osmotically inactive fraction (v_b) of 0.36 (see below). A two-compartment model was also utilized in which the yolk and blastoderm were considered as separate, distinct compartments, of volume and water content appropriate to the 100% epiboly stage. For two compartments, the permeability equations must essentially be solved in duplicate. The fixed and variable parameters of this model are listed in Tables 1 and 2.

Some justification is required for our choice of fixed parameters in the two-compartment model (Table 1). Prior NMR studies [16] show that the yolk and blastoderm were responding differently to cryoprotectants, and this formed the basis for our decision to divide the embryo into a yolk and blastoderm compartment. The volumes and areas of the two compartments were determined from the morphometric data in previous papers [5, 17]. The most difficult parameter to determine was the osmotically inactive fraction of the yolk (v_{by}) and of the blastoderm (v_{bb}). For the blastoderm, we used our estimate of $v_{bb} = 0.2$ from Hagedorn et al. [17]. However, depending on the method of measurement, we obtained v_{by}'s for the yolk ranging from 0.41 to 0.78 [17]. To help chose an appropriate value, we turned to the PG optical shrink data. In some experiments with exposure times up to 225 min in 2 M PG, the embryos were observed to shrink in a linear fashion by 40–50% (data not shown). This large shrinkage requires a large percentage of water (or a small percentage of inactive volume) in the zebrafish embryo. For this reason, we used the lowest yolk value, $v_{by} = 0.41$, suggested by our earlier experiments. Combining the compartment volumes and v_b data yields an overall osmotically inactive volume (v_b) for the embryo of 0.36 (see Table 1).

In either case, it must be understood that the permeability parameters determined are phenomenological parameters characterizing the average response of a very complex structure, and caution should be used in attributing them to any specific membrane. Because of the complexity of this system and the required approximations, none of the determined permeability parameters are considered to be accurate to better than a factor of two.

EM Analysis

We examined the type of cryodamage evident at the level of the electron microscope in various compartments of the zebrafish embryo after vitrification. We chose vitrification as a method because zebrafish embryos are chill-sensitive [4, 5], and the rapid rate of cooling used to vitrify may ultimately increase embryo survival. Embryos at 100% epiboly were immersed into 2 M PG for 2.5 h, then 6 M PG for 2–4 min, drawn into 0.25-ml straws, cooled in liquid nitrogen vapor for 3 min, then plunged into liquid nitrogen for 1–2 min. To thaw, straws were held horizontally at room temperature (22–23°C) for 10 sec, then plunged into room temperature water until thawed (approximately 30 sec). Afterwards, the embryos were diluted by steps into 3 M, 2 M, then 1 M PG for 20 min each. Control embryos were exposed to all chemicals but were not subjected to freezing. To prepare for EM, both experimental and control embryos (n = 3 each) were placed in a fixative (2.5% glutaraldehyde, 1% paraformaldehyde in cacodylate buffer) 10 min after thawing for 2–3 h at 22°C, and then for 1–3 h at 4°C. Embryos were stored for 24 h in cacodylate buffer at 4°C, fixed in 1% osmium tetroxide in cacodylate buffer for 1 h, en bloc stained with 2% uranyl acetate for 1 h, then dehydrated in a series of alcohols (70, 70, 80, 90 and 100, 100, 100% ethyl alcohol) for 5–6 min each, followed by propylene oxide (1:1, 1:2, and 1:3 for 5–6 min each) and 100% propylene oxide for 40 min. Embryos were infiltrated with Spurr's plastic resin (for 18 h), embedded in fresh plastic, and placed in a 70°C oven for polymerization. Sections were cut at 600–800 Å and mounted onto copper grids that were stained for 1.5 min in lead citrate, and then examined using a Zeiss EM10 CA transmission electron microscope.

To evaluate whether the cellular morphology of the frozen and nonfrozen embryos was similar, thin sections were made at three positions (i.e., through the center of the embryo and 200 μm to each side, see Fig. 1B). Then, on each thin section, three areas including the blastoderm and YSL were randomly chosen and scored for intact cells, nuclear membranes, the presence and normal appearance of various organelles (e.g., mitochondria, Golgi bodies, endoplasmic reticulum, etc.), and the presence of yolk droplets (Fig. 1C). In the yolk, the presence of intact membranes and smooth yolk material was assessed. Each intact class of organelle or membrane was given one point for its presence in the tissue. A maximum of 10 points was possible in the blastoderm and the YSL, and two points in the yolk. Mean scores from the yolk, YSL, and blastoderm of each treatment were analyzed with a two-tailed *t*-test and then graphed. Representative areas of the specimens were photographed and printed.

RESULTS

Biophysical Data: Volumetric and NMR

When zebrafish embryos were exposed for long periods of time (i.e., 60 min) to 2 M DMSO or PG, their light microscopic volumes exhibited an approximately linear decrease over time without any re-expansion (Fig. 3). The steady volume decrease observed over the long duration of the experiments suggested that the embryo experienced mostly dehydration with little to no solute permeation. At some point during the dehydrating events, the embryonic structure began to lose integrity. For example, after embryos were immersed in 2 M DMSO for 90–120 min, the blastoderm began to shed cells, and a rupture of the yolk in that area followed shortly thereafter.

NMR spectroscopy allows the solute uptake to be measured directly. When embryos were perfused with a 2 M DMSO solution, DMSO uptake was rapid during the first few minutes, then gradual thereafter (Fig. 4). The response time of the DMSO perfusion system was determined by measuring the NMR signal rise-time in the buffer slice (positioned above the embryos, data not shown). The rise-time

Downloaded from https://academic.oup.com/biolreprod/article/59/5/1240/2741051 by guest on 16 August 2022

of the DMSO signal from 10% to 90% was 2.3 min. This imposed a lower limit on the attainable time resolution of the embryo response to DMSO exposure.

The NMR data suggested some embryo permeability to DMSO, whereas the light microscopic data suggested little embryo permeability to DMSO. At first glance, this presented a somewhat contradictory picture of the permeability within the embryo. In order to estimate the permeability parameters, we analyzed these data with a one- and two-compartment model.

One-Compartment Model

The NMR and optical data were first analyzed with a one-compartment model (Tables 1 and 2) to determine whether this would yield a useful phenomenological model of the embryo. The optical volumetric data gave a water permeability (L_p^s) for 2 M DMSO of 0.007 $\mu m \times min^{-1}atm^{-1}$ and an upper limit to the solute permeability (P_s) of 4×10^{-5} cm/min (Fig. 5A; Table 3). In contrast, the NMR DMSO-uptake data gave a water permeability (L_p^s) of 0.03 $\mu m \times min^{-1}atm^{-1}$ and a P_s of 0.003 cm/min (Fig. 5B). Although good fits were obtained in each case (Fig. 5), the optical and NMR permeability parameters did not agree. Comparing the resultant permeability values (Table 3) reveals a 4-fold difference in L_p values and at least a 75-fold difference in P_s values between the optical and NMR one-compartment fits. Another way to illustrate this discrepancy was to simultaneously fit the optical and NMR data with a single set of parameters (Fig. 5C). This resulted in an intermediate pair of permeability parameters that yielded a poor fit to both the optical and NMR data.

Analysis of the optical volumetric data for embryos immersed in 2 M PG (data from Fig. 3) yielded similar water and solute permeabilities similar to those of DMSO (fit not shown; Table 3).

Two-Compartment Model

The optical and NMR data were also analyzed using a two-compartment model, the blastoderm being one compartment, and the yolk, the second. By fitting these data simultaneously, sufficient constraints were obtained to fit values for L_p^s of the yolk and blastoderm and P_s of the blastoderm, and to find an upper limit for P_s for the yolk. In the presence of 2 M DMSO, the yolk and blastoderm had very similar water permeabilities (i.e., 0.01 and 0.005 $\mu m \times min^{-1}atm^{-1}$, respectively) but different solute permeabilities separated by three orders of magnitude (i.e., $\leq 5 \times 10^{-6}$ and 1.5×10^{-3} cm/min, respectively; Fig. 6, Table 3). Empirically, it was found that the permeability parameters for the yolk were largely fixed by the volumetric data, whereas those for the blastoderm were fixed by the solute uptake data.

Although NMR PG-uptake data could not be obtained, it was still possible to do a two-compartment analysis of the volumetric PG data. As noted above, the volumetric data primarily reflect the response of the yolk. Thus, the yolk permeability parameters are only weakly constrained by the NMR solute uptake data. We made the assumption that the blastoderm water and solute permeabilities in the presence of PG are less than or equal to twice those found for DMSO. With these assumptions, a two-compartment fit to the volumetric PG data for the yolk compartment yielded slightly smaller water and solute permeabilities for PG than for DMSO (Table 3).

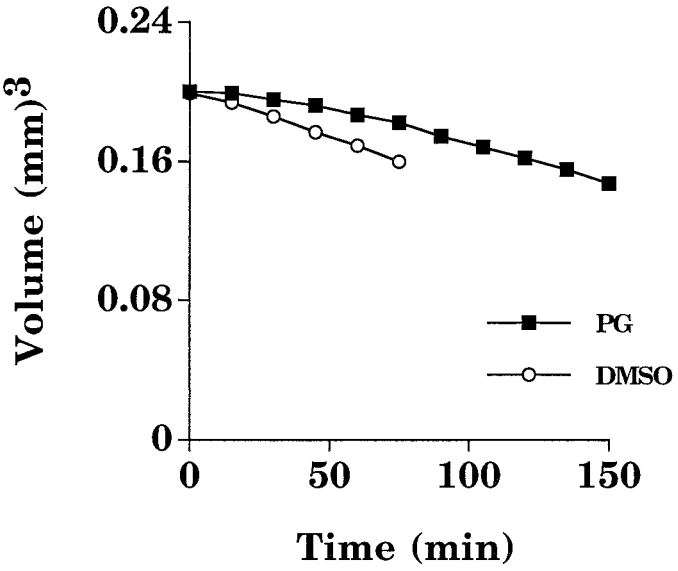

FIG. 3. Volume changes in zebrafish embryo as a function of time in 2 M DMSO (n = 7) and 2 M PG (n = 9) at 22–23°C measured with light microscopy. A decrease of approximately 20% in the averaged volume was observed. The data from each group were averaged and normalized to a standard volume of 0.2 mm^3 for each graph.

Cryodamage

If there is a permeability barrier in the yolk compartment, how might cryopreservation effect the blastoderm, YSL, and yolk? To test this, the embryos were subjected to a vitrification procedure. During freezing, the external solution (6 M PG) surrounding the embryos remained clear, suggesting that the external solution vitrified. All of the frozen embryos (n = 26) died after thawing, whereas 32% of the solution-control embryos (which passed through all solutions, but were not frozen; n = 25) survived and continued to develop. The normal laminar structure of the zebrafish embryo is shown in Figure 7. Control and frozen

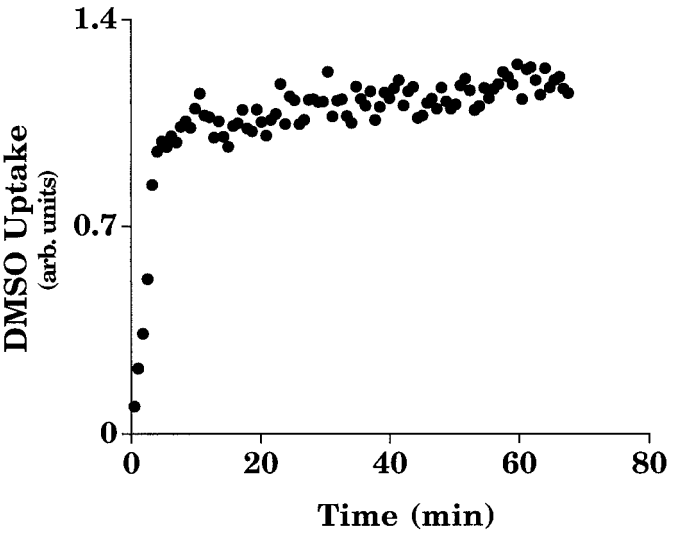

FIG. 4. NMR measured DMSO uptake by embryos at 100% epiboly (21°C). Three measurements were run on samples containing 20 embryos each. The measurements were individually normalized, then averaged. The embryos were perfused with 2 M DMSO beginning at time zero. The observed initial rise time is partially limited by the time required for the perfusate to reach 2 M concentration in the sample chamber.

Downloaded from https://academic.oup.com/biolreprod/article/59/5/1240/2741051 by guest on 16 August 2022

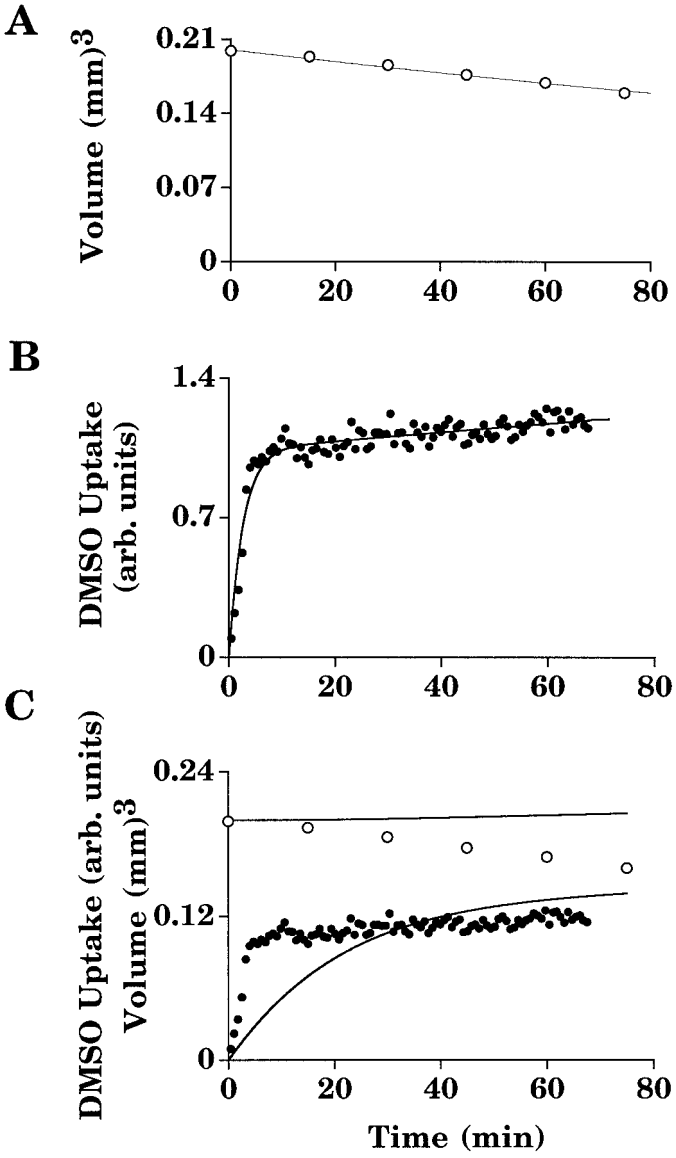

FIG. 5. One-compartment model fit to the zebrafish embryo. Tables 1 and 2 show the fixed parameters used. **A**) The optical volumetric data from Figure 3 (2 M DMSO) were fit with a one-compartment model, which yielded a well-defined value of $L_p^s = 0.007$ μm × min^{-1}atm^{-1}, but only an upper limit of $P_s \leq 4 \times 10^{-5}$ cm/min. The solid curve illustrates an acceptable fit with $P_s = 1 \times 10^{-5}$ cm/min. **B**) The NMR DMSO-uptake data from Figure 4 were fit with a one-compartment model. The solid curve shows a model fit assuming the zebrafish embryo is a single compartment, yielding an $L_p^s = 0.03$ μm × min^{-1}atm^{-1} and $P_s = 0.003$ cm/min. **C**) The optical (open circles) and NMR (solid circles) data were simultaneously fit with a one-compartment model yielding $L_p^s = 0.01$ μm × min^{-1}atm^{-1}, $P_s = 3 \times 10^{-4}$ cm/min, and a very poor fit. Note that the scaling of the NMR data is arbitrary and different from that in Figure 5B.

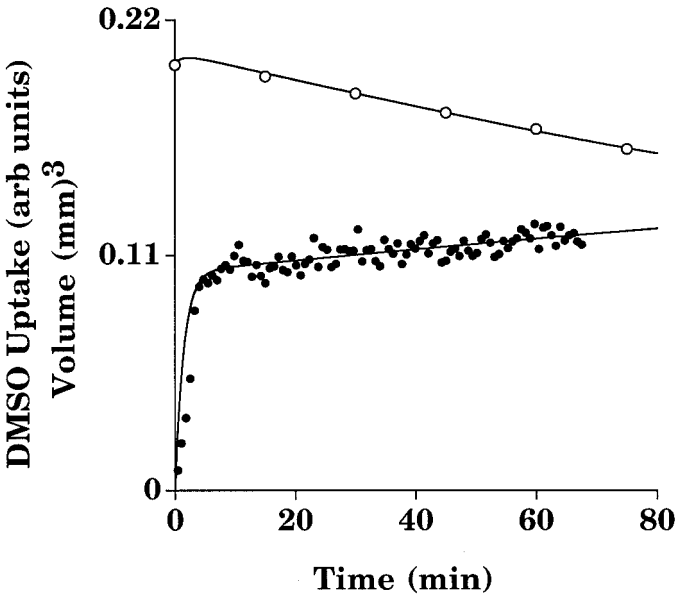

FIG. 6. Two-compartment model fit to the zebrafish embryo in 2 M DMSO at 22–23°C. The experimental optical volume data (in mm^3) are plotted as open circles, and the NMR-measured DMSO uptake (in arbitrary units) are plotted as solid circles. The solid curves are a two-compartment model fit to the combined data using a single set of water and solute permeabilities for the yolk and blastoderm compartments (i.e., $L_{py}^s = 0.01$ μm × min^{-1}atm^{-1}, $L_{pb}^s = 0.005$ μm × min^{-1}atm^{-1}, $P_{sy} = 1 \times 10^{-6}$ cm/min, and $P_{sb} = 0.0015$ cm/min). The data only constrain P_{sy} to $P_{sy} \leq 5 \times 10^{-6}$ cm/min.

embryos were examined and scored at the ultrastructural level to identify areas of the embryo that were damaged. Control embryos showed little or no damage to the blastoderm, yolk, or YSL as a result of the chemical treatment (i.e., cell structures were intact and showed normal morphology; $p \geq 0.05$; Fig. 8). In contrast, experimental embryos exhibited altered morphology only in the YSL ($p \leq 0.05$). Specifically, after freezing, many of the organelles in the YSL were destroyed, and the cellular membrane was destroyed (usually in the area of blastopore closure); some YSL nuclei were present, but the chromatin was congested, and the nuclear membrane was not always intact (Fig. 9). Morphologically, the yolk was not affected by freezing, as the yolk membranes were intact and the yolk contents appeared to be normal. We concluded that cryodamage within the yolk may be tolerated. However, damage to the YSL (the only other major organizing structure related to the yolk) may destroy the integrity of the yolk/YSL compartment, thus leading to the lethal effects observed after thawing.

DISCUSSION

Using a one-compartment model (Fig. 5), we found that no single set of parameters simultaneously fit the optical and NMR data. However, a two-compartment model provided a better fit to the data (Fig. 6). In the presence of DMSO, the yolk and blastoderm compartments had similar water permeabilities but substantially different solute permeabilities. The yolk compartment was essentially impermeable to DMSO ($P_s \leq 5 \times 10^{-6}$ cm/min), whereas the blastoderm compartment had a ''typical'' membrane solute permeability ($P_s = 1.5 \times 10^{-3}$ cm/min). This readily explains the different behavior seen in the DMSO uptake and volumetric experiments. In the volumetric experiments, when the blastoderm cells were exposed to 2 M DMSO, they experienced a rapid shrink/swell response. This is not

TABLE 2. Summary of two-compartment model of zebrafish embryo at 100% epiboly.

	Yolk	Blastoderm	Embryo
Volume (mm^3)	0.15	0.05	0.20
Volume fraction of embryo	0.77	0.23	1.00
Water fraction of compartment	0.59	0.80	0.64
Solids fraction of compartment	0.41	0.20	0.36

Downloaded from https://academic.oup.com/biolreprod/article/59/5/1240/2741051 by guest on 16 August 2022

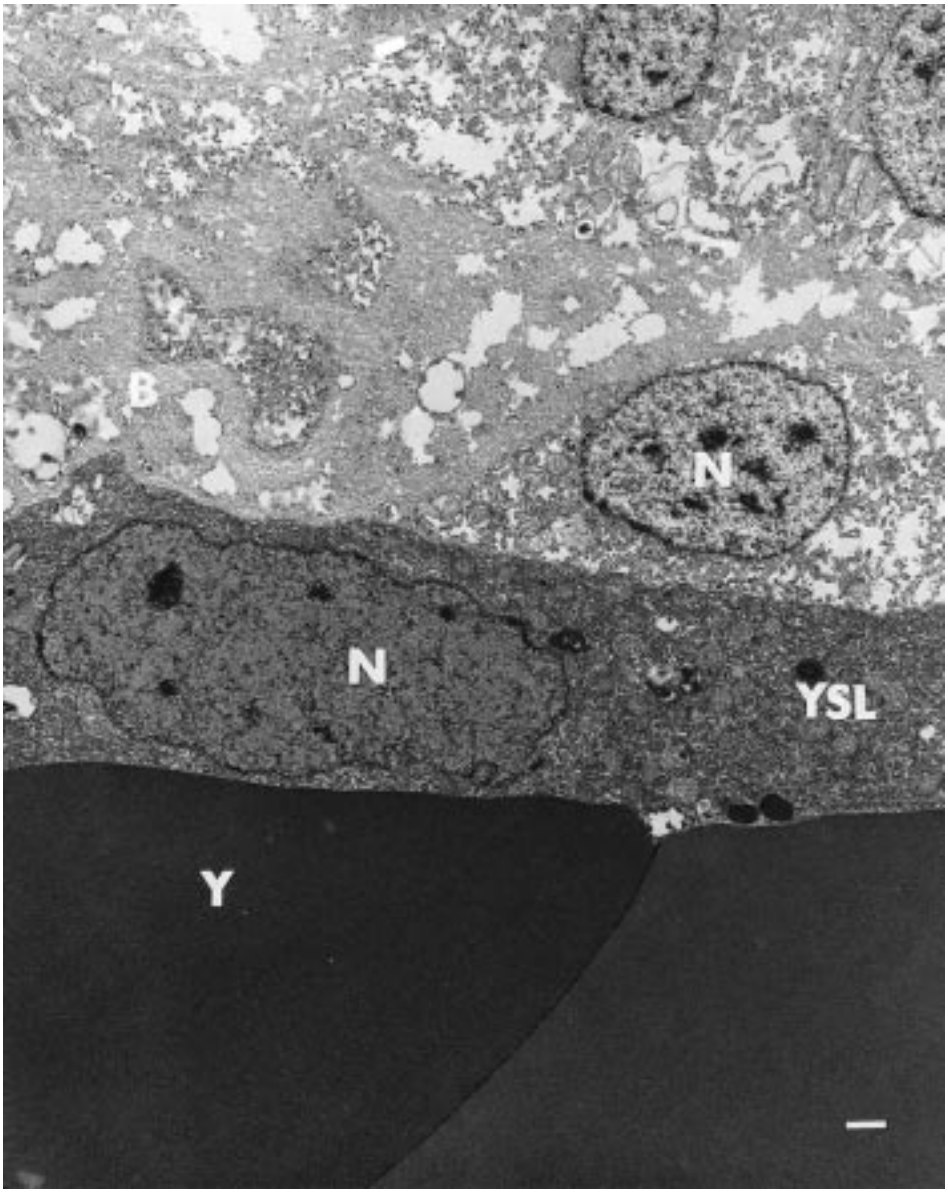

FIG. 7. Control image of the zebrafish embryo at the 3-somite stage showing the normal laminar structure of the blastoderm (B), YSL, and yolk (Y). In all areas, membranes are intact and nuclei (N) are visible in the blastoderm and YSL. The dense, granular appearance of the YSL is due to the abundance of ribosomes. The yolk has a smooth appearance and resides within membrane-bound yolk-vesicles (bar, lower right = 1 μm).

evident in the data, because the shrink/swell response was most likely small and occurred quickly (i.e., between the first and second experimental data points). Since the yolk compartment is essentially impermeable to DMSO, it showed a slow, steady loss of water to the hyperosmotic DMSO environment, yielding a steady decrease in volume, which dominated the volumetric data. In the NMR uptake experiments, primarily the blastoderm was permeable to the DMSO, and the data reflect this response. Initially there was a rapid influx of DMSO due to the large solute gra-

TABLE 3. Permeability parameters of zebrafish embryo exposed to 2 M DMSO at 21°C (NMR experiments), 22–23°C (optical experiments), and 2 M PG at 22–23°C (optical experiments): one- and two-compartment permeability results (L_p^s and P_s) of the optical volume versus time and the NMR uptake versus time data.[a]

Experiment	Solute	L_p^s	P_s	L_{py}^s	L_{pb}^s	P_{sy}	P_{sb}
One-compartment[b]							
Optical volume	DMSO	0.007	$\leq 4 \times 10^{-5}$	—	—	—	—
NMR uptake	DMSO	0.03	0.003	—	—	—	—
Optical volume	PG	0.004	$\leq 5 \times 10^{-6}$	—	—	—	—
Two-compartment[c]							
NMR & optical	DMSO	—	—	0.01	0.005	$\leq 5 \times 10^{-6}$	0.0015
Optical volume[d]	PG	—	—	0.006	≤0.01	$\leq 2 \times 10^{-6}$	≤0.003

[a] The dimensions of L_p^s are micrometers × $min^{-1}atm^{-1}$ and of P_s are cm/min.
[b] Model: one-compartment, two-parameter model.
[c] Model: two-compartment (yolk and blastoderm), two parameter model.
[d] The values of the blastoderm permeability (L_{pb}^s and P_{sb}) could not be calculated and were assumed to be less than twice the values found in the DMSO experiments.

Downloaded from https://academic.oup.com/biolreprod/article/59/5/1240/2741051 by guest on 16 August 2022

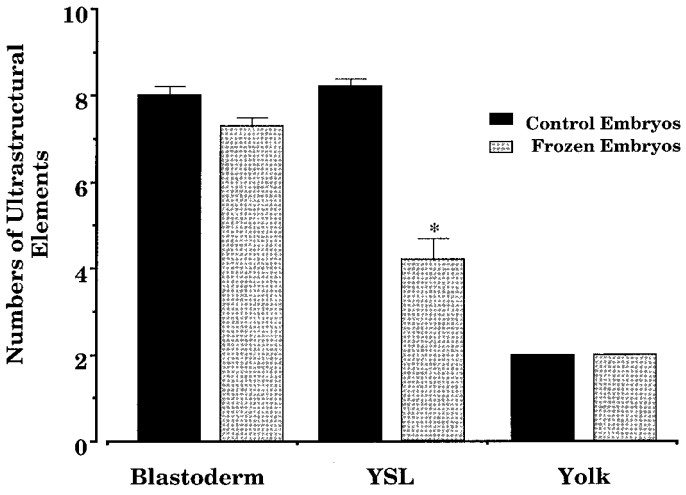

FIG. 8. Histogram quantifying the number of ultrastructural elements in 3-somite embryos after exposing embryos to a solution-control or cryoprotectant, then freezing, and thawing. Only the YSL in the frozen sample showed a loss of structural elements ($*p < 0.05$), whereas the ultrastructure of the blastoderm and the yolk appeared the same in both treatments ($p \geq 0.05$).

dient; however, as equilibrium was approached, the influx of DMSO slowed. Figure 10 shows the individual responses of the two-compartment model and how they combine to yield the observed DMSO uptake and volumetric response.

Of course, one-compartment models are used routinely to characterize single cells. Even in multicellular systems, a one-compartment model may yield useful phenomenological information (e.g., in mouse embryos [19], pancreas [20], and *Drosophila* [21]). A two- or multicompartmental model is only useful if there are sufficient experimental data to characterize the two compartments, and if the responses of the two compartments are so different that a single set of phenomenological parameters do not adequately characterize the system. This is the case with the zebrafish data presented here. The volumetric and DMSO uptake experiments provide a comprehensive data set, and the two putative compartments of the zebrafish embryo (i.e., blastoderm and yolk/YSL) differ by three or more orders of magnitude in their cryoprotectant (DMSO) permeability, 1.5×10^{-3} and $\leq 5 \times 10^{-6}$ cm/min, respectively. In comparison, mouse oocytes in DMSO or PG have $P_s = 0.96$ to 1.4×10^{-3} cm/min [22], and goat oocytes in PG have $P_s = 0.87$

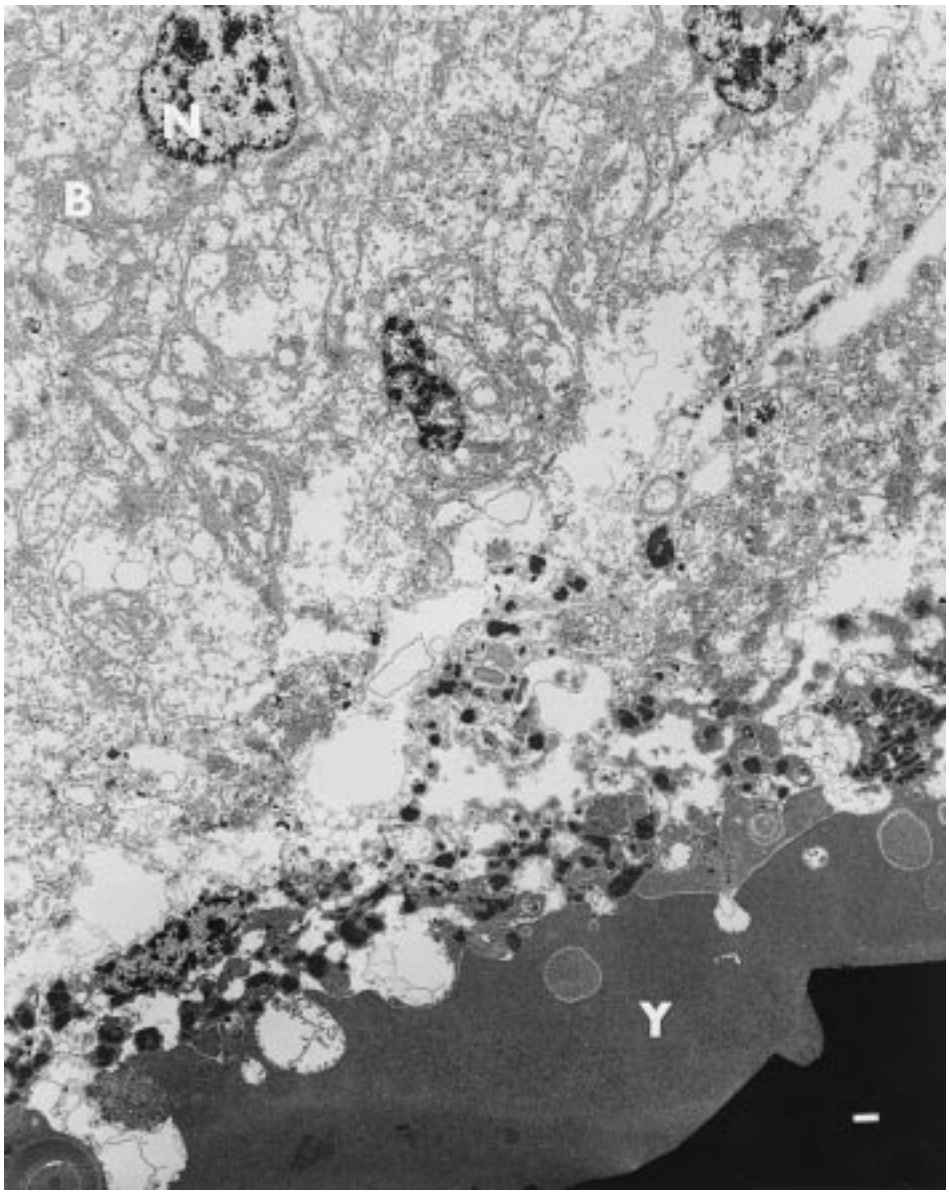

FIG. 9. After freezing and thawing, the ultrastructure of the YSL was destroyed. No clear YSL layer remained as the ribosomal material from the YSL was scattered throughout the blastoderm (B) and yolk (Y). However, the areas not in direct contact with the YSL appeared normal. Most membranes and nuclei (N) of the blastoderm (in the upper part of the figure) and yolk (area not shown) remained intact (bar, lower right = 1 μm).

Downloaded from https://academic.oup.com/biolreprod/article/59/5/1240/2741051 by guest on 16 August 2022

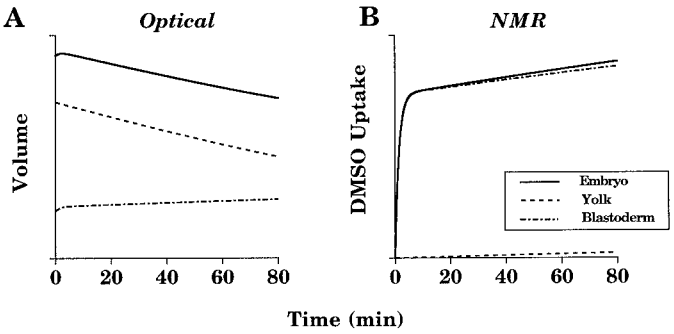

FIG. 10. Two-compartment model simulations showing the response of a zebrafish embryo exposed to 2 M DMSO at room temperature. This illustrates how the response of the each compartment contributes to yield the experimentally observed response of the entire zebrafish embryo. The simulations were generated using the two-compartment parameters shown in Tables 1 and 2 and their permeability values in Table 3. **A**) The two different dashed lines indicate the changing volume of the blastoderm and yolk compartments. Combining these yields the volume of the entire embryo (solid line). This simulation is directly comparable with the optically determined volume versus time data shown in Figure 3. **B**) The two different dashed lines indicate the changing DMSO solute in the blastoderm and yolk compartments. Combining these yields the total DMSO uptake by the embryo (solid line), which is directly comparable with the NMR DMSO uptake data shown in Figure 4.

to 1.2×10^{-3} cm/min [23]. Because the yolk is completely surrounded by the blastoderm at 100% epiboly, it might be argued that the low apparent solute permeability of the yolk compartment simply results from the surrounding layer of blastoderm cells, which block ready access of the extracellular medium to the yolk. However, if this were the case, we would expect the yolk compartment to have a very low water permeability as well. This suggests that the blastoderm does not create the solute permeability barrier around the yolk compartment, but the YSL does.

There is a major difference in the predictions that the one- and two-compartment models make regarding cryopreservation protocols. We modeled the time required for DMSO to reach two thirds of its final concentration (approximately 2 M) within the embryo and yolk for the one- and two-compartment models, respectively, using the upper limits of the solute permeability given in Table 3. The one-compartment model predicted a minimum time of 2.2 h for the embryo to reach the projected DMSO concentration. This is a reasonable treatment time given the constraints of the rapidly developing embryo. However, the two-compartment model predicted a minimum of 9 h for the yolk to reach the projected concentration. This is an unreasonable treatment time, because of toxicity and the large change in development that the embryo would experience by the end of the test period. Clearly, the predictions of the two-compartment model will impose some important constraints on future cryopreservation protocols.

Previously, we measured the water permeability of the zebrafish embryo in the absence of cryoprotectants using optical volumetric methods and a one-compartment model [17]. The value of L_p we obtained at the 100% epiboly stage was 0.05 $\mu m \times min^{-1}atm^{-1}$, and may be compared with our one-compartment analyses of the DMSO and PG optical volumetric data (Table 3). This revealed that L_p dropped by an order of magnitude in the presence of either DMSO or PG and is consistent with a growing body of evidence suggesting that L_p is modified in the presence of permeating cryoprotectants for a variety of membrane types [5, 24, 25]. Clearly, for most cryobiological purposes, it is important to measure membrane water permeability in the presence of proposed cryoprotective solutes. Other investigators have also measured the water permeability of fish embryos in the presence of cryoprotectants. Zhang and Rawson [15] report zebrafish L_ps of 0.10 and 0.17 $\mu m \times min^{-1}atm^{-1}$ in the presence of PG and methanol, respectively. Their permeabilities are more than an order of magnitude larger than our similarly obtained, optical volumetric results. Some of this may be due to a difference in modeling parameters or in the osmolality of the buffer used to make the solutions. Nevertheless, in the presence of solutes, their L_ps appear to be substantially larger than those obtained here.

Previously, we identified the YSL, and not the yolk itself, as the barrier to the movement of cryoprotectant into the yolk [16]. In this study, we have characterized a permeability barrier in the yolk compartment of the zebrafish embryo, but what are the consequences of this barrier to cryopreservation? At the ultrastructural level, the most obvious consequence of our vitrification protocol was a destruction of the YSL surrounding the yolk. This is not to suggest that other, more subtle changes did not occur in the blastoderm and the yolk after the tissue was frozen and thawed. For example, the mere presence of ultrastructural elements within a tissue does not mean they are present in sufficient quantity for normal cell function. A study of serial sections quantifying the number of ultrastructural elements per area of tissue may have shown a clear difference in the blastoderm tissue of the controls and frozen embryos. Additionally, the high concentration of cryoprotectants used in vitrification (approximately 6 M or greater) could have caused a disruption of cytoskeletal elements. Using fluorescent antibodies, Hotamisligil et al. [26] observed a disruption in the actin filaments of the mouse embryo after exposure to 4 M ethylene glycol for more than 10 min. Hypothetically, if little or no cryoprotectant reached the yolk because of the impermeable YSL, ice-crystals may have formed, leading to some type of damage in both the yolk and YSL regions. However, these more subtle issues are moot, because the test vitrification protocol caused the complete destruction of the YSL.

Our ultrastructural experiments suggested that cryodamage led to the death of the embryos, in part because of insufficient cryoprotectant entering the yolk/YSL region. Isotope-uptake experiments have quantified how little cryoprotectant enters the blastoderm, and the yolk in particular. Harvey et al. [10] measured a DMSO concentration in the whole, dechorionated zebrafish embryo of 100 mM after 60 min in 1 M DMSO. After incubating carp embryos in 1.5 M isotope-labeled DMSO for 2 h, Magnus et al. [27] extracted yolk fractions with a micropipette and found approximately 100 mM DMSO. All of these values are well in line with the predictions that the two-compartment model made about the permeability of the zebrafish yolk compartment to DMSO after 2 h (approximately 150 mM) and lends support for the two-compartment model when considering the yolk specifically.

Now that we have characterized and quantified the permeability parameters in the zebrafish embryo, we must examine how we can overcome this permeability barrier to successfully cryopreserve fish embryos. The YSL is a common morphological feature in all teleost fish and will be an important consideration for cryopreservation in most threatened species and for important cultured species, such as catfish, salmonids, tilapia, sturgeon, and striped bass. It is clear that exposure alone may not allow enough cryopro-

Downloaded from https://academic.oup.com/biolreprod/article/59/5/1240/2741051 by guest on 16 August 2022

tectant to enter the yolk for successful cryopreservation. A means for getting cryoprotectant into and past the YSL barrier is required. The vast arsenal of molecular biological methods created for transfecting cells, such as the introduction of pores in the YSL through chemical (e.g., antibiotics) or physical (e.g., electroporation) means, may help overcome this permeability barrier, thus opening the door for successful cryopreservation protocols for fish embryos.

ACKNOWLEDGMENTS

We would like to thank Dr. P. Mazur at the Oak Ridge National Laboratory (Oak Ridge, TN), Dr. S. Blackband at the University of Florida (Gainsville, FL), and Dr. V. Chacko at Johns Hopkins School of Medicine (Baltimore, MD) for their discussion on many of the ideas in this manuscript; Dr. E. Hsu at Duke University Medical Center (Durham, NC) for his insightful comments on the manuscript; and Dr. Lee-Ann Hayek of the Smithsonian Institution (Washington, DC) for statistical assistance.

REFERENCES

1. Rall WF. Recent advances in the cryopreservation of salmonid fishes. In: Cloud JG, Thorgaard GH (eds.), Genetic Conservation of Salmonid Fishes. New York: Plenum Publishing Corporation; 1993: 137–158.
2. Postlethwait JH, Yan Y-L, Gates MA, Horne S, Amores A, Brownlie A, Donovan A, Egan ES, Force A, Gong Z, Goutel C, Fritz A, Kelsh R, Knapik E, Liao E, Paw B, Ransom D, Singer A, Thomson T, Abduljabbar TS, Yelick P, Beier D, Joly J-S, Larhammar D, Rosa F, Westerfield M, Zon LI, Talbot WS. Vertebrate genome evolution and the zebrafish gene map. Nat Genet 1998; 18:345–349.
3. Mommson TP, Walsh PJ. Vitellogenesis and oocyte assembly. In: Hoar WS, Randall DJ, Donaldson EM (eds.), Fish Physiology, vol. XI A. New York: Academic Press; 1988: 348–407.
4. Zhang T, Rawson DM. Studies on chilling sensitivity of zebrafish (*Brachydanio rerio*) embryos. Cryobiology 1995; 32:239–246.
5. Hagedorn M, Kleinhans FW, Wildt DE, Rall WF. Chill sensitivity and cryoprotectant permeability of dechorionated zebrafish embryos, *Brachydanio rerio*. Cryobiology 1997; 34:251–263.
6. Westerfield M. The Zebrafish Book. A Guide for the Laboratory Use of Zebrafish (*Brachydanio rerio*). Eugene, OR: University of Oregon Press; 1993.
7. Kimmel CB, Law RD. Cell lineage of zebrafish blastomeres. II. Formation of the yolk syncytial layer. Dev Biol 1985; 108:86–93.
8. Betchaku T, Trinkhaus JP. Contact relations, surface activity, and cortical microfilaments of marginal cells of the enveloping layer and of the yolk syncytial and yolk cytoplasmic layers of *Fundulus* before and during epiboly. J Exp Zool 1978; 206:381–426.
9. Solnica-Krezel L, Driever W. Microtubule arrays of the zebrafish yolk cell: organization and function during epiboly. Development 1994; 120:2443–2455.
10. Harvey B, Kelley RN, Ashwood-Smith MJ. Permeability of intact and dechorionated zebra fish (*Brachydanio rerio*) embryos to glycerol and dimethyl sulfoxide. Cryobiology 1983; 20:432–439.
11. Harvey B. Cooling of embryonic cells, isolated blastoderms, and intact embryos of the zebra fish *Brachydanio rerio* to minus 196 Celsius. Cryobiology 1983; 20:440–447.
12. Suzuki T, Komada H, Takai R, Arii K, Kozima TT. Relation between toxicity of cryoprotectant DMSO and its concentration in several fish embryos. Fish Sci 1995; 61:193–197.
13. Lubzens E, Ar A, Magnus Y. Steps towards cryopreservation of Japanese ornamental carp embryos: sensitivity to low temperatures and permeation of ^{3}H-dimethyl sulfoxide (DMSO). Aquaculture 1998; (in press).
14. Zhang T, Rawson DM. Feasibility studies on vitrification of intact zebrafish (*Brachydanio rerio*) embryos. Cryobiology 1996; 33:1–13.
15. Zhang T, Rawson DM. Permeability of the vitelline membrane of zebrafish (*Brachydanio rerio*) embryos to methanol and propane-1,2-diol. Cryo Lett 1996; 17:273–280.
16. Hagedorn M, Hsu E, Pilatus U, Wildt DE, Rall WF, Blackband SJ. Magnetic resonance microscopy and spectroscopy reveal kinetics of cryoprotectant permeation in a multicompartmental biological system. Proc Natl Acad Sci USA 1996; 93:7454–7459.
17. Hagedorn M, Kleinhans FW, Freitas R, Liu J, Hsu E, Wildt DE, Rall WF. Water distribution and permeability of zebrafish embryos, *Brachydanio rerio*. J Exp Zool 1997; 278:356–371.
18. Frahm J, Merboldt KB, Haenicke W. Localized proton spectroscopy using stimulated echoes. J Magn Reson 1987; 72:502–508.
19. Jackowski S, Leibo SP, Mazur P. Glycerol permeabilities of fertilized and unfertilized mouse ova. J Exp Zool 1980; 2:329–341.
20. Mazur P, Rajotte RV. Permeability of the 17-day fetal rat pancreas to glycerol and dimethyl sulfoxide. Cryobiology 1981; 18:1–16.
21. Lin T-T, Pitt RE, Steponkus PL. Osmotic behavior of *Drosophila melanogaster* embryos. Cryobiology 1989; 26:453–471.
22. Paynter SJ, Fuller BJ, Shaw RW. Temperature dependence of mature mouse oocyte membrane permeabilities in the presence of cryoprotectant. Cryobiology 1997; 34:122–130.
23. Le Gal F, Gasqui P, Renard JP. Differential osmotic behavior of mammalian oocytes before and after maturation: a quantitative analysis using goat oocytes as a model. Cryobiology 1994; 31:154–170.
24. van Hoek AN, de Jong MD, van Os CH. Effects of dimethyl sulfoxide and mercurial sulfhydryl reagents on water and solute permeability of rat kidney brush border membranes. Biochim Biophys Acta 1990; 1030:203–210.
25. Gilmore JA, McGann LE, Liu J, Gao DY, Peter AT, Kleinhans FW, Critser JK. Effect of cryoprotectant solutes on water permeability of human spermatozoa. Biol Reprod 1995; 53:985–995.
26. Hotamisligil S, Toner M, Powers RD. Changes in membrane integrity, cytoskeletal structure, and developmental potential of murine oocytes after vitrification in ethylene glycol. Biol Reprod 1996; 55:161–168.
27. Magnus Y, Ar A, Lubzens E. Permeability and toxicity of ^{3}H DMSO to developing ornamental carp eggs. In: Proc. Reprod. Physiol. of Fish, 5th Inter. Symp.; 1995; Austin, TX. p. 128.

Downloaded from https://academic.oup.com/biolreprod/article/59/5/1240/2741051 by guest on 16 August 2022